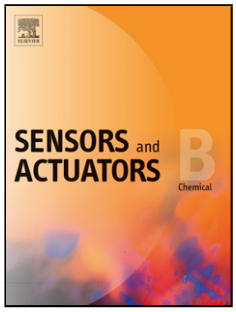

Title: Fluorescent Probes Based on π-Conjugation Modulation between Hemicyanine and Coumarin Moieties for Ratiometric Detection of pH Changes in Live Cells with Visible and Near-infrared Channels

Authors: Shuai Xia, Jianbo Wang, Jianheng Bi, Xiao Wang, Mingxi Fang, Tyler Phillips, Aslan May, Nathan Conner, Marina Tanasova, Fen-Tair Luo, Haiying Liu

PII: S0925-4005(18)30453-2
DOI: https://doi.org/10.1016/j.snb.2018.02.168
Reference: SNB 24263

To appear in: *Sensors and Actuators B*

Received date: 19-12-2017
Revised date: 21-2-2018
Accepted date: 23-2-2018

Please cite this article as: Shuai Xia, Jianbo Wang, Jianheng Bi, Xiao Wang, Mingxi Fang, Tyler Phillips, Aslan May, Nathan Conner, Marina Tanasova, Fen-Tair Luo, Haiying Liu, Fluorescent Probes Based on π-Conjugation Modulation between Hemicyanine and Coumarin Moieties for Ratiometric Detection of pH Changes in Live Cells with Visible and Near-infrared Channels, Sensors and Actuators B: Chemical https://doi.org/10.1016/j.snb.2018.02.168

Fluorescent Probes Based on π-Conjugation Modulation between Hemicyanine and Coumarin Moieties for Ratiometric Detection of pH Changes in Live Cells with Visible and Near-infrared Channels

Shuai Xia,[a] Jianbo Wang,[a,b]* Jianheng Bi,[a] Xiao Wang,[a] Mingxi Fang,[a] Tyler Phillips,[a] Aslan May,[a] Nathan Conner,[a] Marina Tanasova,[a]* Fen-Tair Luo,[c]* and Haiying Liu[a]*

[a]Department of Chemistry, Michigan Technological University, Houghton, MI 49931, E-mail: mtanasov@mtu.edu; hyliu@mtu.edu

[b]College of Biological, Chemical Sciences and Engineering, Jiaxing University, Jiaxing 314001, China. E-mail: wjb4207@mail.ustc.edu.cn

[c]Institute of Chemistry, Academia Sinica, Taipei, Taiwan 11529, Republic of China, E-mail: luoft@gate.sinica.edu.tw

Graphical abstract

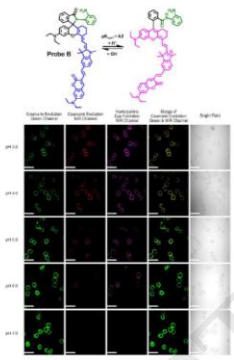

Highlights

- Ratiometric fluorescent probes based on π-conjugation modulation between coumarin and hemicyanine moieties for ratiometric detection of pH changes.
- Morpholine and 1,2-diamine-benzene residues were employed to tune pKa values.
- The probes display ratiometric fluorescence responses to pH from 7.4 to 2.5 and are fully capable of imaging pH changes in live cells in visible and near-infrared channels.
- The platform of the probes can be easily applied to prepare ratiometric fluorescent probes for different analytes.

Abstract

We report two ratiometric fluorescent probes based on π-conjugation modulation between coumarin and hemicyanine moieties for sensitive ratiometric detection of pH alterations in live cells by monitoring visible and near-infrared fluorescence changes. In a π-conjugation modulation strategy, a coumarin dye was conjugated to a near-infrared hemicyanine dye via a vinyl connection while lysosome-targeting morpholine ligand and o-phenylenediamine residue were introduced to the hemicyanine dye to form closed spirolactam ring structures in probes **A** and **B**, respectively. The probes show only visible fluorescence of the coumarin moiety under physiological and basic conditions because the hemicyanine moieties retain their closed spirolactam ring structures. However, decrease of pH to acidic condition causes spirolactam ring opening, and significantly enhances π-conjugation within the probes, thus generating new near-infrared fluorescence peaks of the hemicyanine at 755 nm and 740 nm for probes **A** and **B**, respectively. Moreover, the probes display ratiometric fluorescence response to pH with decreases of the coumarin fluorescence and increases of the hemicyanine fluorescence when pH changes from 7.4 to 2.5. The probes are fully capable of imaging pH changes in live cells with good ratiometric responses in visible and near-infrared channels, and effectively avoid fluorescence blind spots under neutral and basic pH conditions - an issue that typical intensity-based pH fluorescent probes run into. The probe design platform reported herein can be easily applied to prepare a variety of ratiometric fluorescent probes for detection of biological thiols, metal ions, reactive oxygen and nitrogen species by introducing appropriate functional groups to hemicyanine moiety.

Keywords: Fluorescent probe, Ratiometric imaging, near-infrared emission, pH, live cells

1. Introduction

Ratiometric fluorescence imaging offers reliability in quantitative and comparative analyses and effectively overcome variations in the emission intensity, concentration, and compartmental localization of intensity-based fluorescent probes.[1-9] As a result, it has been commonly applied to study highly dynamic intracellular ion, voltage or pH changes. Common approaches to achieve ratiometric fluorescence imaging are to employ Forster Resonance Energy Transfer (FRET) or a through-bond energy transfer (TBET) from a fluorophore donor to a fluorophore acceptor.[10-12] The FRET strategy requires a spectral overlap between the donor emission and the acceptor absorption, which significantly limits choices of the donor and acceptor fluorophore pairs. In contrast, the TBET approach can effectively overcome this limitation, and offer multiple choices for the donor and acceptor fluorophore pairs. Other ratiometric fluorescent probes are based on π-conjugation modulation of fluorophores in response to

analytes.[13-15] Most of the reported ratiometric fluorescent probes are based on Rhodamine acceptors in FRET and TBET strategies, which possess less than 600 nm in the acceptor emission. Therefore, it remains a challenging task, particularly for imaging of lysosomal pH in live cells, to develop ratiometric fluorescent probes with high turn-on fluorescence, large dynamic range, large pseudo-Stokes shifts, photodamage-free near-infrared imaging of living organisms, low autofluorescence interference from biological samples, and highly selective and sensitive ratiometric responses with well-defined dual excitation and emission capability. Although a number of fluorescent probes have been developed for pH detection,[14-41] pH ratiometric fluorescent probes are still limited, especially those with near-infrared emission.

In this paper, we present a simple but effective π-conjugation modulation strategy to construct fluorescent probes (**A** and **B**) for ratiometric detection of pH changes. The design of probe **A** is based on conjugating a coumarin fluorophore to a hemicyanine fluorophore via a vinyl connection and introducing a lysosome-targeting morpholine residue form a closed spirolactam structure of the hemicyanine (Scheme 1). In order to increase pK_a of the probe **B**, *o*-phenylenediamine residue was introduced to hemicyanine moiety. In neutral or basic condition, the probe shows very strong fluorescence of the coumarin fluorophore, and can effectively overcome blind fluorescence imaging encountered for typical intensity-based pH fluorescent probes. This outcome results from no fluorescence of the closed spirolactam structures of the hemicyanine moieties under basic and neutral pH conditions. Gradual decrease of pH from 7.4 to 2.0 causes ratiometric fluorescence responses of probes with the decrease in the coumarin fluorescence and increase in the hemicyanine fluorescence due to the acid-mediated opening of the spirolactam ring and the subsequent enhancement of π-conjugation. The probes show ratiometric response to pH changes in live cells with moderate decrease of the coumarin fluorescence and increase of hemicyanine fluorescence. This probe design strategy can offer a general approach to construct a variety of ratiometric fluorescent probes to detect biological thiols, metal ions, reactive oxygen and nitrogen species by introducing appropriate sensing ligands to the hemicyanine fluorophores with unique spirolactam ring structures.

2. Materials and Methods

2.1 Instrumentation

400 MHz Varian Unity Inova NMR spectrophotometer instrument was employed to collect ^{1}H NMR and ^{13}C NMR spectra in $CDCl_3$ and CD_3OD solutions. Solvent residual peaks (^{1}H: δ 7.26 for $CDCl_3$, δ 3.31

for CD_3OD; ^{13}C: δ 77.3 for $CDCl_3$) were used as internal standards in ppm to define chemical shifts (*δ*) of intermediates and probe. Double focusing magnetic mass spectrometer, fast atom bombardment (FAB) ionization mass spectrometer, or matrix-assisted laser desorption/ionization time of flight mass spectrometer were used determine high-resolution mass spectrometer data (HRMS). Absorption and fluorescence spectra were conducted by using Per-kin Elmer Lambda 35 UV/VIS spectrometer and Jobin Yvon Fluoromax-4 spectrofluorometer, respectively.

2.2 Cell Culture and fluorescence imaging

HeLa cells were purchased from ATCC (Manassas, VA). Cells grown for a minimum of five passages were used in all experiments. The Cells were incubated in a 5% CO_2 humidified incubator at 37 °C and typically passaged with sub-cultivation of 1:3 every two days. For confocal imaging, HeLa cells were seeded into the 35 mm glass-bottom culture dishes (MatTek, MA) and allowed to grow for 1-2 days to reach 70–90% confluence. After 24 h of incubation, the cell culture medium was replaced by freshly prepared serum-free medium with 1, 5, 10, 20 μM of the probe **A** for 1 h. The cells were incubated further with 50 nM LysoTracker red (Thermo-Fisher) for 30 min to confirm the specific targeting of our probe **A** to lysosomes in HeLa cells. Live cell images were taken by a confocal fluorescence microscope (Olympus IX 81). The excitation wavelength of the coumarin is 405 nm and the images were collected at 500 – 550 nm (green channel) and 725 – 775 nm (NIR channel). The excitation wavelength of the hemicyanine dye is 635 nm and the images were collected at 725 – 775 nm (NIR channel). The excitation wavelength of the LysoTracker red is 559 nm and the images were collected at 575 – 625 nm.

2.3 Live cell fluorescence imaging at different intracellular pH values

HeLa cells were seeded into the 35 mm glass-bottom culture dishes (MatTek, MA) and allowed to grow for 1-2 days to reach 70–90% confluence. After 24 h of incubation, HeLa Cells were treated with probe **A** or **B** (15 μM concentrations) at 37 °C for 30 min, followed by rinsing twice with PBS buffer. Cells were then treated with nigericin (5 μg/mL) in buffers with pH values at 3.0, 4.0, 5.0, 6.0, and 7.0 for 30 min to equilibrate the intracellular and extracellular pH. Live cell images were taken by a confocal fluorescence microscope (Olympus IX 81).

2.4 Cell cytotoxicity assay

The cytotoxicity of the probe against HeLa cells was measured by using the standard MTS assay. Cells were seeded into the 96-well cell culture plate at 5×10^3/well in complete medium (DMEM containing 10% fetal bovine serum (FBS)). After growing for 24 h at 37 °C under 5% CO_2 and removal of

the medium, cells were incubated with the probes with concentrations ranging from 0, 2, 5, 10, 15 to 20 μM in fresh culture medium, 100 μL/well) for 48 h at 37 °C under 5% CO_2. The probe solutions were replaced with the fresh culture medium (80 μL/well), and CellTiter 96® Aq_{ueous} (20 μL/well) was added to evaluate cell viability. After incubation for 2 h, the cell viability was determined by measuring the light absorbance at 490 nm with a microplate reader (BioTek ELx800). Untreated cells were used as controls. Percent (%) cell viability was calculated by comparing the absorbance of the control cells to that of treated cells. Data were summarized as a plot where each data point represents an average of three wells.

2.5 Materials

Unless specifically indicated, all reagents and solvents were bought from commercial suppliers and were used without further purification. Compounds **3**, **4** and **8** were prepared and characterized according to the reported procedures (Supporting information).

Compound 5: To the mixture of compound **3** (0.48 g, 1 mmol) and **4** (0.42 g, 1 mmol) in Ac_2O (15 ml) was added KOAc (50 mg) and the reaction was heated at 60 °C for 1 h. The reaction mixture was concentrated under reduced pressure, and the residue partitioned between water (25 ml) and dichloromethane. The organic layer was separated, the combined organic extracts were dried over Na_2SO_4, filtered, and concentrated. The residue was purified by flash column using dichloromethane and methanol to obtain the compound **4a** as green solid (0.47 g, 58%).^{1}H NMR (400M, CD_3OD) δ 8.55 (d, *J* = 13.6 Hz, 1H), 8.15 (d, *J* = 5.6 Hz, 1H), 7.80 (d, *J* = 1.6 Hz, 1H), 7.69 – 7.66 (m, 2H), 7.61 (t, *J* = 7.2 Hz, 1H), 7.20 (d, *J* = 7.2 Hz, 1H), 7.02 (d, *J* = 8.4 Hz, 1H), 6.83 (s, 2H), 6.73 (s, 1H), 6.04 (d, *J* = 13.6 Hz, 1H), 3.58 – 3.52 (q, *J* = 7.2 Hz, 4H), 3.52 (s, 3H), 2.67 – 2.65 (m, 2H), 2.37 – 2.34 (m, 2H), 1.81 – 1.78 (m, 2H), 1.76 (s, 6H), 1.23 (t, *J* = 7.2 Hz, 6H); ^{13}C NMR (100 MHz, CD_3OD) δ 171.3, 163.7, 156.5, 155.9, 152.7, 143.3, 143.1, 140.4, 137.5, 131.7, 131.3, 129.2, 128.9, 128.8, 121.1, 116.6, 114.2, 113.0, 112.1, 98.3, 95.3, 86.9, 44.9, 30.3, 27.5, 26.6, 24.2, 20.6, 11.6. HRMS (ESI): calculated for $C_{37}H_{38}IN_2O_3^+$ [M] $^+$, 685.1922; found, 685.1920.

Compound 7: To the solution of compound **5** (350 mg, 0.5 mmol) in dry dichloromethane (15 ml) was added dicyclohexylcarbodiimide (DCC) (103 mg, 0.5 mmol) and *N*-hydroxy-succinimide (NHS) (69 mg, 0.6 mmol) under a nitrogen atmosphere at room temperature. When the mixture was stirred for 30 min, 4-(2-aminoethyl)morpholine (compound **6**, 98 mg, 0.75 mmol) was added and the reaction was stirred overnight. After the mixture was washed with water (2 × 20 mL), the organic layer was collected, dried over anhydrous Na_2SO_4 and filtered. The filtrate was concentrated under reduced pressure. The residue

was purified by flash column chromatography using ethyl acetate and hexane as the eluent, to afford probe as pray solid. (130 mg, 33%). ^{1}H NMR (400M, $CDCl_3$) δ 7.82 (d, *J* = 7.2 Hz, 1H), 7.46 – 7.36 (m, 5H), 7.14 (d, *J* = 7.2 Hz, 1H), 6.35 (t, *J* = 8.0 Hz, 1H), 6.33 – 6.28 (m, 2H), 6.25 – 6.22 (m, 1H), 5.35 (d, *J* = 12.8 Hz, 1H), 3.58 (t, *J* = 4.4 Hz, 4H), 3.44 – 3.38 (m, 1H), 3.34 – 3.30 (q, *J* = 7.2 Hz, 4H), 3.27 – 3.24 (m, 1H), 3.08 (s, 3H), 2.59 – 2.55 (m, 2H), 2.40 – 2.33 (m, 6H), 2.23 – 2.16 (m, 2H), 1.68 (s, 3H), 1.67 (s, 3H), 1.60 – 1.57 (m, 2H), 1.14 (t, *J* = 7.2 Hz, 6H); ^{13}C NMR (100 MHz, $CDCl_3$) δ 168.5, 156.7, 153.0, 151.7, 148.8, 148.0, 145.3, 141.7, 136.5, 132.3, 130.7, 128.9, 128.3, 123.6, 123.0, 121.4, 119.2, 108.6, 108.0, 105.5, 104.5, 97.9, 92.9, 80.5, 67.2, 66.9, 56.7, 53.7, 45.6, 44.6, 37.1, 29.4, 28.5, 28.4, 25.5, 23.2, 22.4, 12.7. HRMS (ESI): calculated for $C_{43}H_{50}IN_4O_3$ $[M+H]^+$, 797.2928; found, 797.2925.

Probe A: To the solution of compound **7** (70 mg, 89 μmol) in DMF (6 mL) were added the palladium acetate (4 mg, 18 μmol), compound **8** (33 mg, 134 μmol), tri(*o*-tolyl)phosphine (11 mg, 35 μmol), and Et_3N (3 ml). The mixture was heated at 90°C under argon atmosphere overnight. After completion of the reaction (monitored by LC-MS), the reaction was concentrated under reduced pressure and the residue purified by flash column chromatography using dichloromethane and methanol as the eluent. Probe **A** was isolated as red solid (46 mg, 56%). ^{1}H NMR (400M, $CDCl_3$) δ 7.83 (d, *J* = 7.2 Hz, 1H), 7.66 (s, 1H), 7.52 – 7.41 (m, 4H), 7.34 (d, *J* = 16.4 Hz, 1H), 7.27 – 7.24 (m, 2H), 7.17 – 7.15 (m, 1H), 7.02 (d, *J* = 16.4 Hz, 1H), 6.59 – 6.54 (m, 2H), 6.50 (d, *J* = 2.4 Hz, 1H), 6.34 – 6.32 (m, 1H), 6.26 – 6.23 (m, 1H), 5.38 (d, *J* = 12.4 Hz, 1H), 3.60 (t, *J* = 4.4 Hz, 4H), 3.43 – 3.38 (m, 5H), 3.37 – 3.32 (q, *J* = 7.2 Hz, 4H), 3.30 – 3.26 (m, 1H), 3.15 (s, 3H), 2.61 – 2.57 (m, 2H), 2.38 – 2.34 (m, 6H), 2.24 – 2.18 (m, 2H), 1.74 (s, 3H), 1.73 (s, 3H), 1.63 – 1.57 (m, 2H), 1.23 – 1.13 (m, 12H); ^{13}C NMR (100 MHz, $CDCl_3$) δ 168.5, 162.1, 157.7, 155.5, 153.0, 151.7, 150.3, 148.9, 148.1, 145.4, 139.8, 136.1, 130.2, 129.5, 128.9, 128.3, 127.9, 123.6, 123.0, 120.9, 119.5, 119.3, 119.2, 118.7, 109.5, 109.3, 108.6, 105.8, 105.4, 104.1, 97.9, 97.5, 92.9, 67.2, 66.9, 56.7, 53.7, 45.5, 45.1, 44.6, 37.1, 29.9, 29.5, 28.6, 28.5, 25.5, 23.2, 22.4, 12.7, 12.7. HRMS (ESI): calculated for $C_{58}H_{66}N_5O_5$ $[M+H]^+$, 912.5064; found, 912.5067.

Compound 9: To the solution of compound **7** (250 mg, 0.36 mmol) in 1,2-dichloroethane (20 mL) was added phosphorous oxychloride (220 mg, 1.46 mmol) under a nitrogen atmosphere. The reaction was refluxed for 2 h and the solvent was evaporated under vacuum. Dry acetonitrile (20 mL) was added to the residue, and followed by adding 1, 2-diaminobenzene (9) (0.12 g, 1.0 mmol) and triethylamine (0.5 mL). The mixture was stirred was stirred overnight. After the mixture was washed with water (2 × 20 mL), the organic layer was collected, dried over anhydrous Na_2SO_4, filtered and concentrated under reduced pressure. The residue was purified by flash column chromatography using ethyl acetate and hexane as the eluent, to afford probe as yellow solid (120 mg, 53%). ^{1}H NMR (400M, $CDCl_3$) δ 7.95 (d, *J* =

7.2 Hz, 1H), 7.51 – 7.45 (m, 2H), 7.40 (d, *J* = 8.4 Hz, 1H), 7.36 (s, 1H), 7.26 (d, *J* = 12.8 Hz, 1H), 7.22 (d, *J* = 7.6 Hz, 1H), 6.96 (t, *J* = 8.0 Hz, 1H), 6.65 (d, *J* = 8.0 Hz, 1H), 6.59 (d, *J* = 8.8 Hz, 1H), 6.53 (t, *J* = 6.4 Hz, 1H), 6.34 (d, *J* = 8.0 Hz, 1H), 6.30 (d, *J* = 8.8 Hz, 1H), 6.25 (s, 1H), 5.32 (d, *J* = 12.4 Hz, 1H), 3.79 (s, 2H), 3.36 – 3.31 (q, *J* = 7.2 Hz, 4H), 3.05 (s, 3H), 2.59 – 2.56 (m, 1H), 2.35 – 2.31 (m, 1H), 2.09 – 2.06 (m, 2H), 1.64 (s, 6H), 1.62 – 1.58 (m, 2H), 1.16 (t, *J* = 7.2 Hz, 6H); ^{13}C NMR (100 MHz, $CDCl_3$) δ 166.9, 156.4, 153.3, 152.2, 148.9, 148.0, 145.3, 144.1, 141.7, 136.5, 132.6, 131.6, 130.6, 128.8, 128.4, 123.4, 123.9, 123.5, 121.7, 118.9, 118.8, 118.1, 108.6, 108.0, 105.0, 98.2, 93.2, 80.4, 70.8, 45.6, 44.6, 29.5, 28.7, 28.4, 25.6, 24.1, 22.4, 12.9. MS (ESI): calculated for $C_{43}H_{44}IN_4O_2$ $[M+H]^+$, 775.2; found, 775.3.

Probe B: The procedure was similar to the way of synthesizing of the probe **A** using compound 7 (100 mg, 0.13 mmol) as starting materials and probe **B** was obtained as red solid (70 mg, 63%). ^{1}H NMR (400M, $CDCl_3$) δ 7.95 (d, *J* = 6.8 Hz, 1H), 7.64 (s, 1H), 7.54 – 7.45 (m, 3H), 7.40 (d, *J* = 1.6 Hz, 1H), 7.35 – 7.31 (m, 2H), 7.27 – 7.24 (m, 1H), 7.23 – 7.22 (m, 1H), 7.00 (d, *J* = 16.4 Hz, 1H), 6.99 – 6.95 (m, 1H), 7.66 (d, *J* = 7.6 Hz, 1H), 6.59 – 6.45 (m, 6H), 6.31 – 6.27 (m, 2H), 5.34 (d, *J* = 12.4 Hz, 1H), 3.78 (s, 2H), 3.42 – 3.37 (q, *J* = 7.2 Hz, 4H), 3.37 – 3.32 (q, *J* = 7.2 Hz, 4H), 3.11 (s, 3H), 2.60 – 2.57 (m, 1H), 2.35 – 2.31 (m, 1H), 2.08 – 2.05 (m, 2H), 1.69 (s, 6H), 1.63 – 1.58 (m, 2H), 1.21 – 1.16 (m, 12H); ^{13}C NMR (100 MHz, $CDCl_3$) δ 166.9, 162.0, 157.3, 155.4, 153.3, 152.3, 150.2, 148.9, 148.2, 145.4, 144.1, 139.7, 136.0, 132.6, 131.6, 130.2, 129.5, 128.7, 128.4, 127.8, 123.9, 123.5, 121.3, 119.2, 118.9, 118.6, 118.1, 109.5, 109.3, 108.5, 105.8, 104.6, 98.2, 97.5, 93.0, 70.9, 45.5, 45.1, 44.7, 29.5, 28.8, 28.5, 25.6, 24.1, 22.4, 12.9, 12.8. MS (ESI): calculated for $C_{58}H_{60}N_5O_4$ $[M+H]^+$, 890.5; found, 890.5.

3. Results and Discussions

3.1. Synthetic approach

The design and synthesis of the fluorescent probe **A** and **B** are outlined in Scheme **2**. The rational design was based on π-conjugation modulation between two fluorophores in response to pH to achieve ratiometric fluorescence responses of the probe to pH changes. We chose visible emissive coumarin and near-infrared emissive hemicyanine fluorophores to construct a ratiometric fluorescent probe because both fluorophores have excellent photostability, high molar absorption activity, and good fluorescence quantum yield.[33, 38, 42, 43] In order to specifically target lysosome in live cells, morpholine residue was introduced to hemicyanine dye (**5**) to form a closed spirolactam ring structure, affording hemicyanine dye **7**. π-Conjugation between the coumarin and hemicyanine fluorophores via a vinyl connection was achieved by using a palladium-catalyzed Heck coupling reaction between iodo-functionalized hemicyanine (**7**) and vinyl-functionalized coumarin (**8**) so that the probe **A** could respond

to pH changes through π-conjugation modulation between two fluorophores. Iodo-functionalized hemicyanine dye (**5**) was prepared by condensation reaction of compound **3** with 5-iodo-1,2,3,3-tetramethyl-3*H*-indol-1-ium iodide (**4**). In order to increase the pK_a of probe **B**, 1,2-diaminobenzene residue was introduced to hemicyanine moiety to form a closed spirolactam ring by using the same approach as to prepare probe **A** (Scheme 2).

3.2 Optical responses of intermediate 7, probe A and probe B to pH changes

We investigated the pH influence on the absorption properties of the intermediate **7**, probes **A** and **B** in 10 mM citrate buffer containing 40% ethanol. At neutral or basic pH, intermediate **7** shows absorption peak at 380 nm with a closed spirolactam ring structure. Increasing the acidity of the solution from pH 7.0 to 2.0 results in the appearance and increase of a new peak at 723 nm, corresponding to absorption of hemicyanine dye with a spirolactam ring opening structure. Hemicyanine absorption (715 nm) shows The 8 nm red-shift with the presence of the iodo group at hemicyanine dye.[33, 38] Under the neutral and basic conditions, probes **A** and **B** only display broad absorption peaks of coumarin moieties at 475 nm, and 450 nm because the hemicyanine moieties retain closed spirolactam ring structure (Figure 1). Decrease of pH from 7.0 to 2.5 leads to the appearance of new near-infrared absorption peaks at 745 nm and 735 nm for probes **A** and **B**, respectively. The intensity of the near-infrared absorption peak increases with pH decrease from 7.0 to 2.5. Compared with the reported absorption peak of typical hemicyanine dyes at 715 nm under acidic condition,[33, 38] π-conjugation of hemicyanine with coumarin causes red shifts in the absorption peaks of hemicyanine moieties by 22 nm for probe **A**, 12 nm for probe **B** at acidic pH**,** respectively. Furthermore, probes **A** and **B** molar display absorption coefficients of 4.1×10^4 and 3.3×10^4 $mol^{-1}cm^{-1}$ at pH 2.5 responding to the hemicyanine moiety absorption, respectively, indicating that conjugation of the coumarin dye to hemicyanine dye enhances molar absorptivity of the probes.

We evaluated pH effect on fluorescence spectra of the probes **A** and **B** in 10 mM citrate buffer containing 40% ethanol. At pH 7.0, probes **A** and **B** shows no fluorescence of the hemicyanine moieties and fluorescence peak of coumarin moieties at 528 nm and 515 nm with fluorescence quantum yields of 26.0% and 23.5% at the excitation of 420 nm, respectively (Figure 2 and 3). However, probes **A** and **B** exhibit significant increase of hemicyanine fluorescence at 755 nm and 740 nm under excitation of 680 nm, respectively, because pH decrease from 7.0 to 2.5 promotes spirolactam ring opening of the hemicyanine moieties and significantly enhances π-conjugation of the probes. We employed the Henderson–Hasselbach-type mass action equation to calculate pK_{cycl} values of probes **A** and **B** related to

the spirolactam ring opening of the hemicyanine moieties. The pH 4.2 and 4.8 were identified as the equilibrium pH for the spirolactam ring opening for probes **A** and **B**, respectively (Figure 4). Fluorescence quantum yields of coumarin and hemicyanine moieties at pH 3.0 were calculated to be 16.6% and 1.6% at excitation of 420 nm for probe **A**, and 16.0% and 1.3% for probe **B**, respectively. Fluorescence quantum yields of hemicyanine moieties at pH 3.0 is calculated to be 8.3% for probe **A**, and 7.9% for probe **B** at excitation of 680 nm. Both probes **A** and **B** also display ratiometric responses to pH changes from 7.0 to 2.5 with a moderate decrease in the coumarin fluorescence and increase in the hemicyanine fluorescence. We tested whether probes **A** and **B** could respond to pH changes reversibly by measuring fluorescence changes in the coumarin and hemicyanine fluorescence. Probes **A** and **B** displayed reversible responses to pH changes from pH 7.0 to pH 2.5 with ratiometric fluorescence changes in the hemicyanine over coumarin fluorescence (Figure S11).

3.3 The selectivity of fluorescent probe A to the pH over metal ions.

We investigated the selectivity of the probes **A** and **B** to pH over 50 µM metal ions such as Zn^{2+}, Pb^{2+}, Fe^{2+}, Hg^{2+}, Cd^{2+}, Ca^{2+}, Mn^{2+}, Ni^{2+}, Mg^{2+}, Cu^{2+}, Co^{2+}, Na^{+} and K^{+} ions in 10 mM citrate buffer containing 40% ethanol (Figures S12-S15). The results show that the presence of different metal ions does not cause any significant fluorescence changes of the coumarin and hemicyanine moieties at both pH 7.6 and 2.4, indicating that the probes exhibit excellent selectivity to pH over metal ions.

3.4. Photostability of the fluorescent probes A and B.

We examined the photostability of probes **A** and **B** through their continuous excitation at 420 nm with 10-min intervals in 10 mM citrate buffers containing 5 µM probes **A** and **B** in 40% ethanol. Probe **A** shows good photostability with its coumarin fluorescence decrease by 1.0% at pH 7.6 and 2.5% at pH 2.4 and hemicyanine fluorescence decrease by 3.5% at pH 2.4 under 3-hour excitation at 420 nm (Figure S16). Probe **B** also displays excellent photostability with its coumarin fluorescence decrease by 1.3% at pH 7.6 and 2.1% at pH 2.4 and hemicyanine fluorescence decrease by 2.8% at pH 2.4 under 3-hour excitation at 420 nm (Figure S17).

.5. Cytotoxicity of the fluorescent probes A and B.

The MTS assay was used to investigate the cytotoxicity of probes to live cells using HeLa cells (Figure 5). Incubation of HeLa cells with the different concentrations of probes **A** and **B** showed that the cell viability was higher than 70% even at a concentration of 20 µM. Overall, the 15 µM test concentrations of probes **A** and **B** appear to be almost non-cytotoxic for HeLa cells.

3.6. Fluorescence imaging of pH in live cells.

We studied whether probe **A** could image the intracellular pH by conducting live (HeLa) cell imaging with different probe concentrations. The morpholine residue was used to allow the probe to specifically target acidic lysosomes with pH around 4.5 in live cells. We incubated cells in the media containing probe and LysoTracker red to confirm whether our probe and LysoTracker red stay in the same cellular compartments. In HeLa cells, the probe **A** shows strong fluorescence of coumarin moiety and moderate fluorescence of hemicyanine moiety at 10 μM concentration with coumarin excitation at 420 nm. The probe exhibits stronger fluorescence of hemicyanine moiety with the same probe concentration at hemicyanine excitation. Also, fluorescence intensities of both coumarin and hemicyanine moieties increase significantly with the probe concentration. The co-localization analysis of the probe with the commercial LysoTracker red based on the Pearson's coefficient gave a value of 0.85 or higher, indicating that probe **A** and LysoTracker Red exist in the same cellular compartment (Figure 6 and 7).

After demonstrating that the probe **A** selectively targets and stains lysosomes in live cells, we investigated whether the probe could respond to pH changes in live cells. We incubated HeLa cells with the probe in the media adjusted to pH values from 3.0 to 7.0 and used 5 μg/mL nigericin (H^+/K^+ ionophore) to equilibrate the intracellular and extracellular pH. After incubation, the very strong fluorescence of the coumarin moiety at pH 7.0 was observed. The presence of coumarin fluorescence allows overcoming blind fluorescence imaging spots at basic or neutral pH, an issue that most Rhodamine-based pH fluorescent probes encounter. Upon changing the pH from 7.0 to 3.0, ratiometric fluorescence response to pH changes was measured with the gradual coumarin fluorescence decrease and hemicyanine fluorescence increase at the excitation of 420 nm. The probe **A** also shows ratiometric responses to pH changes from 3.0 to 7.0 with fluorescence imaging color changes from yellow to deep green in the merge images of green and NIR fluorescence channels at excitation of the coumarin moiety. The fluorescence intensity of the hemicyanine moiety in the purple channel also gradually increased with the decrease in pH from 7.0 to 3.0 (Figure 8). Probe **B** displays similar ratiometric responses to pH changes in live cells as probe **A** does Figure 9), but it possesses higher pK_a than probe **A** because moderate fluorescence intensity of hemicyanine moiety can still be observed at pH 6.0 (Figure 9). Increase of pK_a of probe **B** arises from introduction steric hindrance of o-phenylenediamine residue to hemicyanine moiety to form spirolactam structure. Probes A and B display ratiometric fluorescence responses to pH changes in live cells (Figure 100 as they do in buffer solutions (Figures 2 and 3).

Conclusion

In summary, we present two fluorescent probes with different pK_a values for ratiometric detection of pH changes in live cells by conjugating coumarin moiety to the near-infrared hemicyanine moiety through a vinyl connection and introducing morpholine and *o*-diaminebenzene residues to the hemicyanine to form a closed spirolactam structures, respectively. The probes show ratiometric fluorescence responses with coumarin fluorescence decreases and hemicyanine fluorescence increases to the pH changes from 7.0 to 3.0. The π-conjugation modulation between coumarin and hemicyanine moieties used in this probe design offers an effective way to construct a wide variety of ratiometric fluorescent probes to determine metal ions, biological thiols, reactive nitrogen and oxygen species after functionalization of the hemicyanine moiety with appropriate sensing ligands.

Acknowledgements

The research reported in this publication was supported by the National Institute of General Medical Sciences of the National Institutes of Health under Award Number R15GM114751 (to H.Y. Liu) and China Scholarship Council (to J.B. Wang).

References

[1] R. Kawagoe, I. Takashima, S. Uchinomiya, A. Ojida, Reversible ratiometric detection of highly reactive hydropersulfides using a FRET-based dual emission fluorescent probe, Chem Sci, 8(2017) 1134-40.
[2] Y.Y. Zhang, S.L. Li, Z.W. Zhao, Using Nanoliposomes To Construct a FRET-Based Ratiometric Fluorescent Probe for Sensing Intracellular pH Values, Anal Chem, 88(2016) 12380-5.
[3] X.T. Jia, Q.Q. Chen, Y.F. Yang, Y. Tang, R. Wang, Y.F. Xu, et al., FRET-Based Mito-Specific Fluorescent Probe for Ratiometric Detection and Imaging of Endogenous Peroxynitrite: Dyad of Cy3 and Cy5, J Am Chem Soc, 138(2016) 10778-81.
[4] G.J. Song, S.Y. Bai, X. Dai, X.Q. Cao, B.X. Zhao, A ratiometric lysosomal pH probe based on the imidazo 1,5-a pyridine-rhodamine FRET and ICT system, RSC Adv, 6(2016) 41317-22.
[5] Y.R. Zhang, N. Meng, J.Y. Miao, B.X. Zhao, A Ratiometric Fluorescent Probe Based on a Through-Bond Energy Transfer (TBET) System for Imaging HOCl in Living Cells, Chem Eur J, 21(2015) 19058-63.
[6] L.W. He, B.L. Dong, Y. Liu, W.Y. Lin, Fluorescent chemosensors manipulated by dual/triple interplaying sensing mechanisms, Chem Soc Rev, 45(2016) 6449-61.
[7] R.Q. Zhang, F.Y. Yan, Y.C. Huang, D.P. Kong, Q.H. Ye, J.X. Xu, et al., Rhodamine-based ratiometric fluorescent probes based on excitation energy transfer mechanisms: construction and applications in ratiometric sensing, RSC Adv, 6(2016) 50732-60.
[8] L. Yuan, W.Y. Lin, K.B. Zheng, S.S. Zhu, FRET-Based Small-Molecule Fluorescent Probes: Rational Design and Bioimaging Applications, Accounts of Chemical Research, 46(2013) 1462-73.
[9] J.L. Fan, M.M. Hu, P. Zhan, X.J. Peng, Energy transfer cassettes based on organic fluorophores: construction and applications in ratiometric sensing, Chem Soc Rev, 42(2013) 29-43.
[10] M. Dimura, T.O. Peulen, C.A. Hanke, A. Prakash, H. Gohlke, C.A.M. Seidel, Quantitative FRET studies and integrative modeling unravel the structure and dynamics of biomolecular systems, Curr Opin Struct Biol, 40(2016) 163-85.
[11] C.E. Rowland, C.W. Brown, I.L. Medintz, J.B. Delehanty, Intracellular FRET-based probes: a review, Methods and Applications in Fluorescence, 3(2015).
[12] N. Kumar, V. Bhalla, M. Kumar, Resonance energy transfer-based fluorescent probes for Hg2+, Cu2+ and Fe2+/Fe3+ ions, Analyst, 139(2014) 543-58.
[13] J. Zhang, S. Zhu, L. Valenzano, F.-T. Luo, H.Y. Liu, BODIPY-based Ratiometric Fluorescent Probes for Sensitive and Selective Sensing of Cyanide Ion, RCS Advances, 3(2012) 68-72.
[14] Q.Q. Wan, S.M. Chen, W. Shi, L.H. Li, H.M. Ma, Lysosomal pH Rise during Heat Shock Monitored by a Lysosome-Targeting Near-Infrared Ratiometric Fluorescent Probe, Angew Chem Int Ed, 53(2014) 10916-20.
[15] Y.H. Li, Y.J. Wang, S. Yang, Y.R. Zhao, L. Yuan, J. Zheng, et al., Hemicyanine-based High Resolution Ratiometric near-Infrared Fluorescent Probe for Monitoring pH Changes in Vivo, Anal Chem, 87(2015) 2495-503.
[16] Z.J. Diwu, C.S. Chen, C.L. Zhang, D.H. Klaubert, R.P. Haugland, A novel acidotropic pH indicator and its potential application in labeling acidic organelles of live cells, Chem Biol, 6(1999) 411-8.
[17] H.S. Lv, J. Liu, J. Zhao, B.X. Zhao, J.Y. Miao, Highly selective and sensitive pH-responsive fluorescent probe in living Hela and HUVEC cells, Sens Actuator B-Chem, 177(2013) 956-63.
[18] H. Zhu, J.L. Fan, Q.L. Xu, H.L. Li, J.Y. Wang, P. Gao, et al., Imaging of lysosomal pH changes with a fluorescent sensor containing a novel lysosome-locating group, Chem Commun, 48(2012) 11766-8.
[19] Z. Li, Y.L. Song, Y.H. Yang, L. Yang, X.H. Huang, J.H. Han, et al., Rhodamine-deoxylactam functionalized poly styrene-alter-(maleic acid) s as lysosome activatable probes for intraoperative detection of tumors, Chem Sci, 3(2012) 2941-8.
[20] L.Q. Ying, B.P. Branchaud, Selective labeling and monitoring pH changes of lysosomes in living cells with fluorogenic pH sensors, Bioorg Med Chem Lett, 21(2011) 3546-9.

[21] D.G. Smith, B.K. McMahon, R. Pal, D. Parker, Live cell imaging of lysosomal pH changes with pH responsive ratiometric lanthanide probes, Chem Commun, 48(2012) 8520-2.
[22] L.J. Ma, W.G. Cao, J.L. Liu, D.Y. Deng, Y.Q. Wu, Y.H. Yan, et al., A highly selective and sensitive fluorescence dual-responsive pH probe in water, Sens Actuator B-Chem, 169(2012) 243-7.
[23] F. Galindo, M.I. Burguete, L. Vigara, S.V. Luis, N. Kabir, J. Gavrilovic, et al., Synthetic macrocyclic peptidomimetics as tunable pH probes for the fluorescence imaging of acidic organelles in live cells, Angew Chem Int Ed, 44(2005) 6504-8.
[24] H.M. DePedro, P. Urayama, Using LysoSensor Yellow/Blue DND-160 to sense acidic pH under high hydrostatic pressures, Anal Biochem, 384(2009) 359-61.
[25] T. Hasegawa, Y. Kondo, Y. Koizumi, T. Sugiyama, A. Takeda, S. Ito, et al., A highly sensitive probe detecting low pH area of HeLa cells based on rhodamine B modified beta-cyclodextrins, Biorg Med Chem, 17(2009) 6015-9.
[26] H.J. Lin, P. Herman, J.S. Kang, J.R. Lakowicz, Fluorescence lifetime characterization of novel low-pH probes, Anal Biochem, 294(2001) 118-25.
[27] L. Wang, Y. Xiao, W.M. Tian, L.Z. Deng, Activatable Rotor for Quantifying Lysosomal Viscosity in Living Cells, J Am Chem Soc, 135(2013) 2903-6.
[28] B.L. Dong, X.Z. Song, C. Wang, X.Q. Kong, Y.H. Tang, W.Y. Lin, Dual Site-Controlled and Lysosome-Targeted Intramolecular Charge Transfer-Photoinduced Electron Transfer-Fluorescence Resonance Energy Transfer Fluorescent Probe for Monitoring pH Changes in Living Cells, Anal Chem, 88(2016) 4085-91.
[29] Q.Q. Wang, L.Y. Zhou, L.P. Qiu, D.Q. Lu, Y.X. Wu, X.B. Zhang, An efficient ratiometric fluorescent probe for tracking dynamic changes in lysosomal pH, Analyst, 140(2015) 5563-9.
[30] J.T. Zhang, M. Yang, W. Mazi, K. Adhikari, M.X. Fang, F. Xie, et al., Unusual Fluorescent Responses of Morpholine-Functionalized Fluorescent Probes to pH via Manipulation of BODIPY's HOMO and LUMO Energy Orbitals for Intracellular pH Detection, ACS Sens, 1(2016) 158-65.
[31] J.T. Zhang, M. Yang, C. Li, N. Dorh, F. Xie, F.T. Luo, et al., Near-infrared fluorescent probes based on piperazine-functionalized BODIPY dyes for sensitive detection of lysosomal pH, Journal of Materials Chemistry B, 3(2015) 2173-84.
[32] M. Schaferling, Nanoparticle-based luminescent probes for intracellular sensing and imaging of pH, Wiley Interdisciplinary Reviews-Nanomedicine and Nanobiotechnology, 8(2016) 378-413.
[33] S.W. Zhang, T.H. Chen, H.M. Lee, J.H. Bi, A. Ghosh, M.X. Fang, et al., Luminescent Probes for Sensitive Detection of pH Changes in Live Cells through Two Near-Infrared Luminescence Channels, ACS Sens, 2(2017) 924-31.
[34] G.L. Niu, P.P. Zhang, W.M. Liu, M.Q. Wang, H.Y. Zhang, J.S. Wu, et al., Near-Infrared Probe Based on Rhodamine Derivative for Highly Sensitive and Selective Lysosomal pH Tracking, Anal Chem, 89(2017) 1922-9.
[35] M. Grossi, M. Morgunova, S. Cheung, D. Scholz, E. Conroy, M. Terrile, et al., Lysosome triggered near-infrared fluorescence imaging of cellular trafficking processes in real time, Nature Communications, 7(2016).
[36] X.B. Song, M.Y. Hu, C. Wang, Y. Xiao, Near-infrared fluorescent probes with higher quantum yields and neutral pK(a) values for the evaluation of intracellular pH, RSC Adv, 6(2016) 69641-6.
[37] P. Li, H.B. Xiao, Y.F. Cheng, W. Zhang, F. Huang, W. Zhang, et al., A near-infrared-emitting fluorescent probe for monitoring mitochondrial pH, Chem Commun, 50(2014) 7184-7.
[38] G.K. Vegesna, J. Janjanam, J.H. Bi, F.T. Luo, J.T. Zhang, C. Olds, et al., pH-activatable near-infrared fluorescent probes for detection of lysosomal pH inside living cells, Journal of Materials Chemistry B, 2(2014) 4500-8.
[39] J.T. Hou, W.X. Ren, K. Li, J. Seo, A. Sharma, X.Q. Yu, et al., Fluorescent bioimaging of pH: from design to applications, Chem Soc Rev, 46(2017) 2076-90.

[40] J. Yin, Y. Hu, J. Yoon, Fluorescent probes and bioimaging: alkali metals, alkaline earth metals and pH, Chem Soc Rev, 44(2015) 4619-44.
[41] W. Shi, X.H. Li, H.M. Ma, Fluorescent probes and nanoparticles for intracellular sensing of pH values, Methods and Applications in Fluorescence, 2(2014).
[42] Q.S. Zheng, L.D. Lavis, Development of photostable fluorophores for molecular imaging, Curr Opin Chem Biol, 39(2017) 32-8.
[43] K.P. Barot, S.V. Jain, L. Kremer, S. Singh, M.D. Ghate, Recent advances and therapeutic journey of coumarins: current status and perspectives, Med Chem Res, 24(2015) 2771-98.

Shuai Xia received B.S. and M.S. degrees in pharmaceutical analysis at Southwest University, China. He is a Ph.D candidate in chemistry department, Michigan Technological University. His current research focuses on fluorescent probes to detect pH and metal ions *in vivo* and *in vitro*.

Jianbo Wang received his Ph.D from University of Science and Technology of China in 2012. After he worked at WuXi AppTec Co., Ltd for a year, he joined in College of Biological, Chemical Sciences and Engineering, Jiaxing University in 2013. He is an associate professor and his current research interests are the design and synthesis of florescent sensors.

Jianheng Bi received his bachelors of applied chemistry from East Normal University in 2010. He pursues his Ph.D. study at Michigan Technological University. He is developing and characterizing fluorescent probes and theranostics for detection of pH changes in live cells and for cancer imaging and chemotherapy.

Xiao Wang pursues his Ph.D. study at Michigan Technological University after he obtained a Master degree at Harbin Institute of Technology. He is developing theranostics for cancer imaging and chemotherapy.

Mingxi Fang is currently studying at Michigan Technological University for a Ph.D. degree of chemistry. His research interests focus on design, synthesis and characterization of near infrared fluorescent probes for celling imaging application.

Tyler Philips is an undergraduate student at Michigan Technological University pursuing a bachelor's degree in Chemistry.

Aslan May is an undergraduate student at Michigan Technological University pursuing a bachelor's degree in Chemistry.

Nathan Conner is an undergraduate student at Michigan Technological University pursuing a bachelor's degree in Chemistry.

Marina Tanasova received her Ph.D. degree in Chemistry from Michigan State University in 2009. She did her postdoctoral work in Medicinal Chemistry and Toxicology at the University of Minnesota in 2009-2010 and then at Swiss Federal Institute of Technology in 2010-2013. She is currently an Assistant Professor of Chemistry at Michigan Technological University. Dr. Tanasova research interests are in developing fluorescent molecular probes to target and modulate biological mechanisms towards cancer detection and therapy.

Fen-Tair Luo received his Ph.D. degree at Purdue University in 1984. He did one-year postdoctoral research at Stanford University. He became an associate research fellow at the Institute of Chemistry in Academia Sinica in 1985 and was promoted to a research fellow in 1991. His research interests include exploratory organometallics in organic syntheses. He is also interested in doing research in supertorrefaction, a process of making biocarbon materials from biomass in molten salt, to have high throughput production of biocarbons.

Haiying Liu received his Ph.D. degree at Fudan University in 1995. He did postdoctoral research at University of Miami in 1998, and at University of Pittsburgh from 1999 to 2002. He is a full professor in Department of Chemistry, Michigan Technological University. His research interests include design and

synthesis of fluorescent probes and theranostics for detection of metal ions, biothiols, enzymes, proteins, reactive oxygen and nitrogen species, cancer imaging and therapy.

Figure 1. Absorbance spectra of 5 μM intermediate **7** (left), probe **A** (middle) and probe **B** (right) in 10 mM citrate buffer containing 40% EtOH.

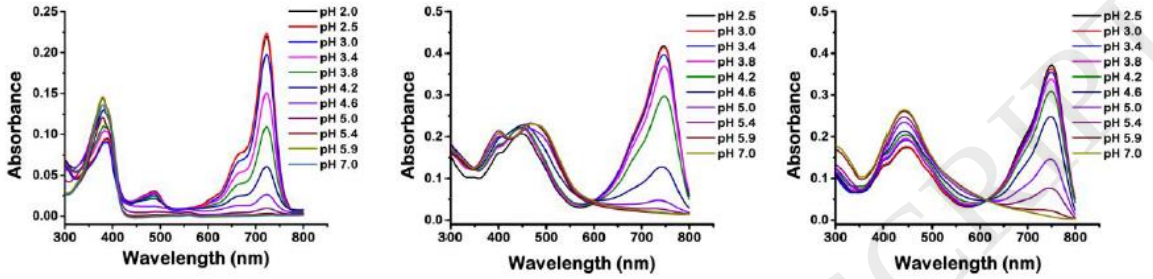

Figure 2. Fluorescence spectra of 5 μM probe **A** in 10 mM citrate buffer containing 40% EtOH at excitation of 420 nm (left), 420 nm (right) and 680 nm (right), respectively; pH dependent fluorescence ratios of hemicyanine acceptor ($I_{755\ nm}$) to coumarin donor ($I_{528\ nm}$) at excitation of 420 nm (middle).

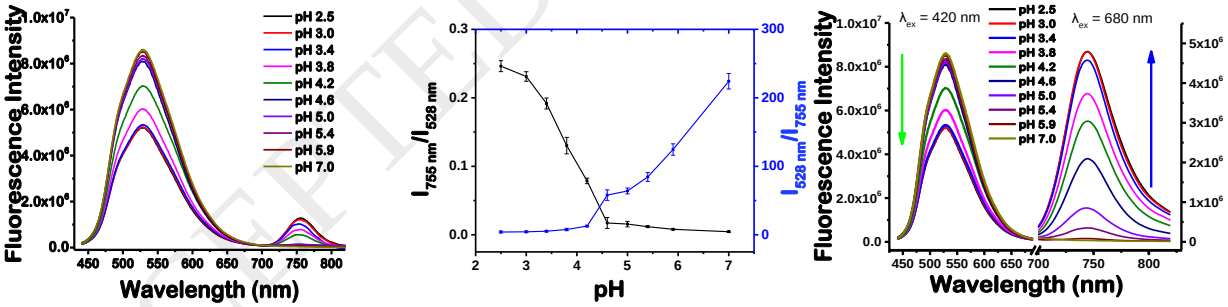

Figure 3. Fluorescence spectra of 5 μM probe **B** in 10 mM citrate buffer containing 40% EtOH at excitation of 420 nm (left), 420 nm (right) and 680 nm (right), respectively; pH dependent fluorescence ratios of hemicyanine acceptor ($I_{740\ nm}$) to coumarin donor ($I_{515\ nm}$) at excitation of 420 nm (middle).

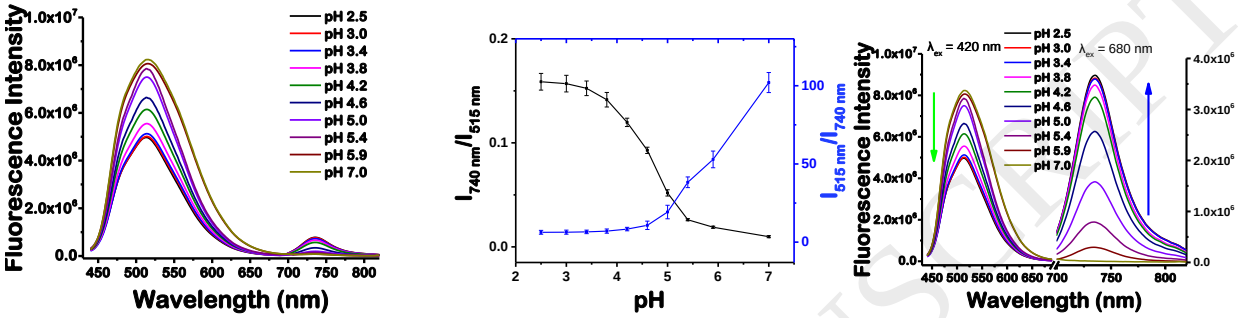

Figure 4. Plots of fluorescent intensity of 5 μM probe **A** (left) at 755 nm and probe **B** (right) at 740 nm versus pH at 680 nm excitation with three repeated measurements.

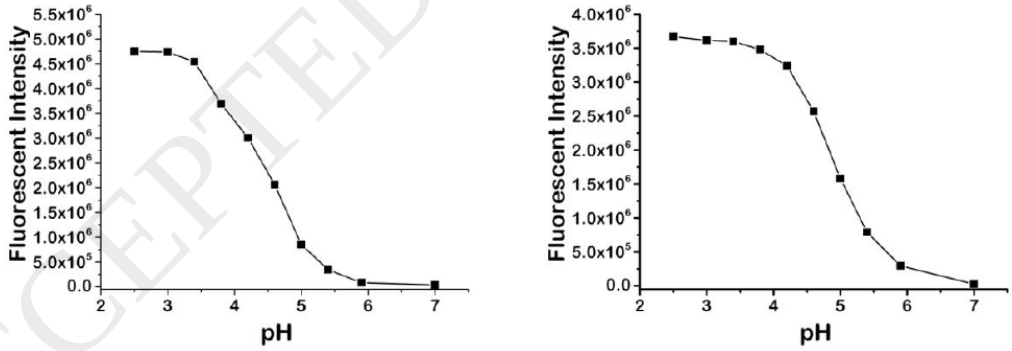

Figure 5. Cytotoxicity and cell proliferation of probes **A** and **B** conducted by MTS assay. HeLa cells were incubated with 2, 5, 10, 15, and 20 µM of probes for 48 h, and cell viability was measured by adding MTS reagent and measuring at 490 nm. The absorbance measured at 490 nm was directly proportional to the cell viability and was normalized to control cells in the absence of probes.

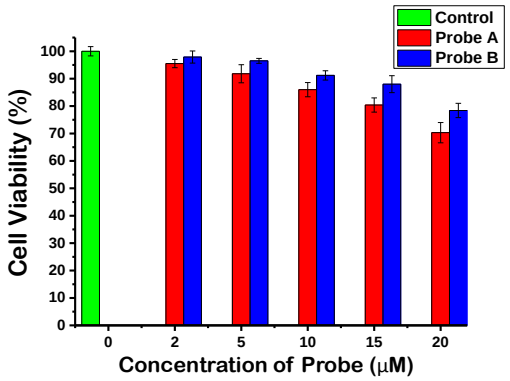

Figure 6: Fluorescence images of HeLa cells incubated with different concentrations of probe **A** in the presence of LysoTracker Red. Images were acquired using the confocal fluorescence microscope at 60 X magnification. Scale Bar: 50 µM

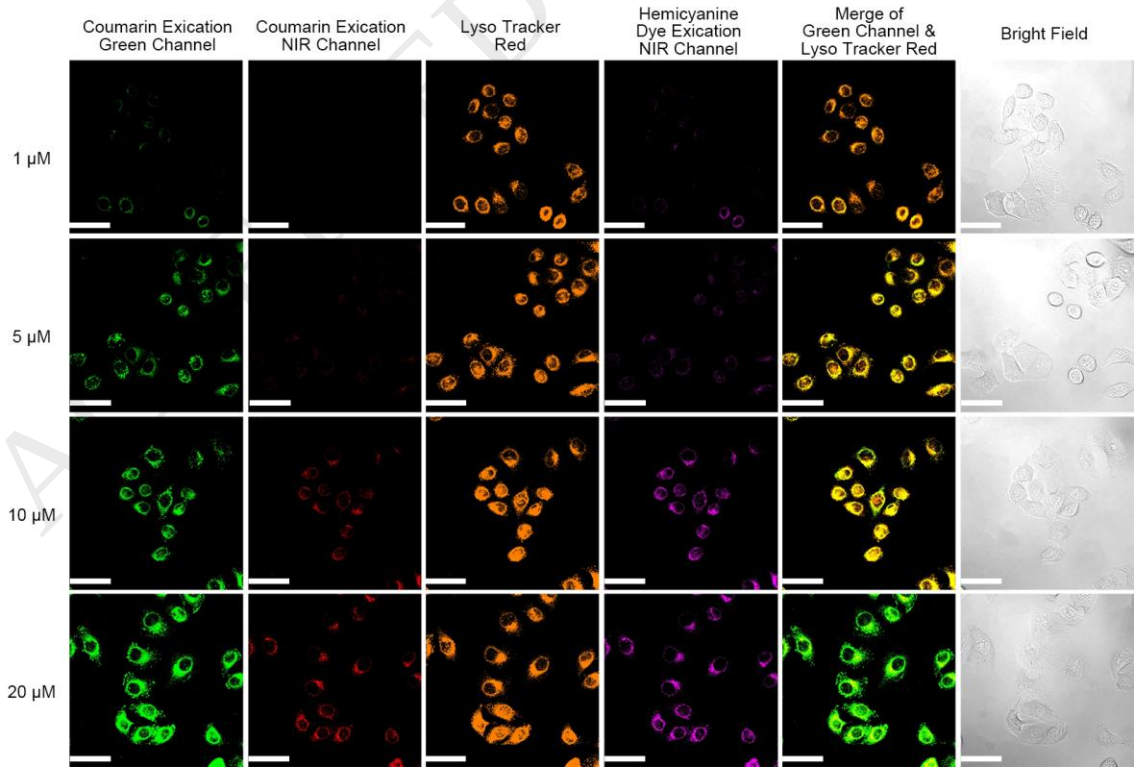

Figure 7: Enlarged fluorescence images of HeLa cells incubated with different concentrations of probe **A** in the presence of LysoTracker Red.

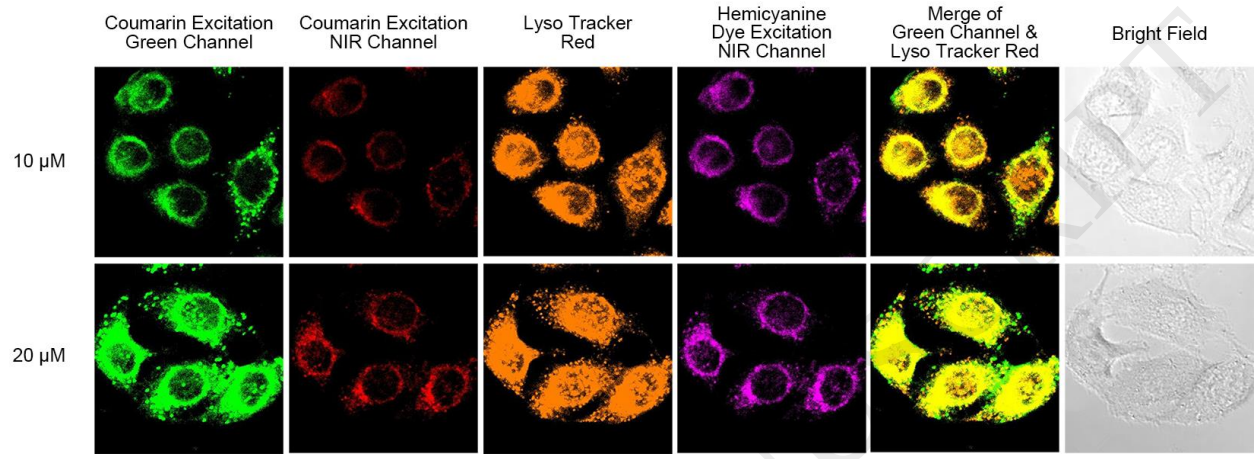

Figure 8: Fluorescence images of HeLa cells incubated with 15 µM fluorescent probe **A**. HeLa cells were incubated with 15 µM probe **A** at the pH ranging from pH 3.0 to 7.0 in presence of 5 µg/mL nigericin. Images were acquired using the confocal fluorescence microscope at 60 X magnification. Scale Bar: 50 µM

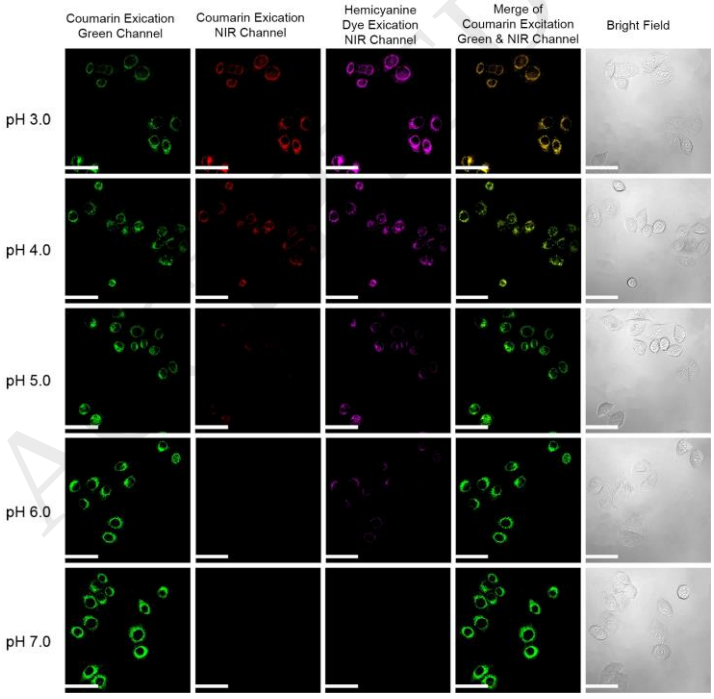

Figure 9: Fluorescence images of HeLa cells incubated with 15 µM fluorescent probe **B**. HeLa cells were incubated with 15 µM probe **B** at the pH ranging from pH 3.0 to 7.0 in presence of 5 µg/mL nigericin. Images were acquired using the confocal fluorescence microscope at 60 X magnification. Scale Bar: 50 µM

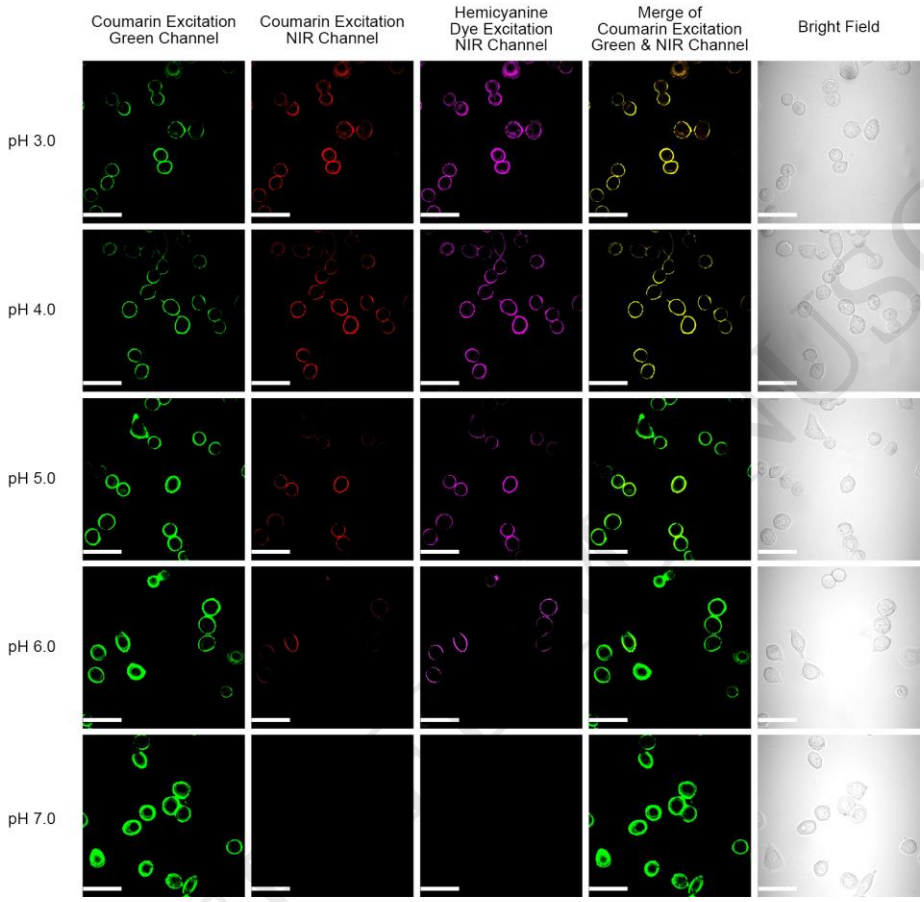

Figure 10: Fluorescence intensity of probe **A** (left) and probe **B** (right) in the HeLa cells obtained from statistical analysis of the confocal imaging in figures 8 and 9.

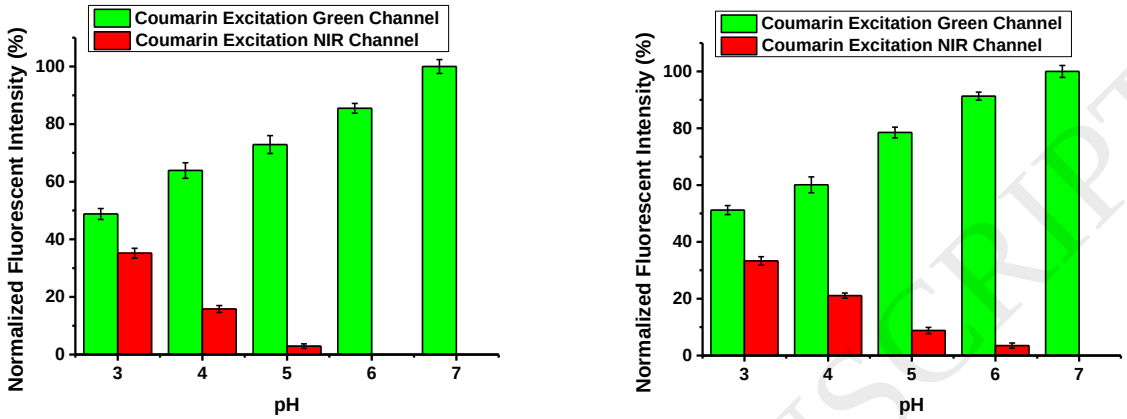

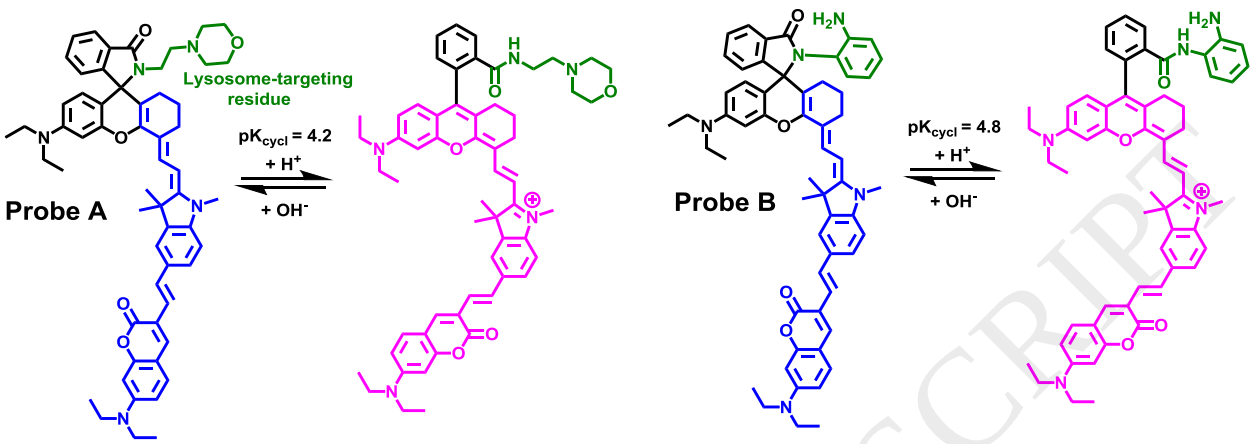

Scheme 1. Chemical structure response of fluorescent probes to pH changes with π-conjugation changes.

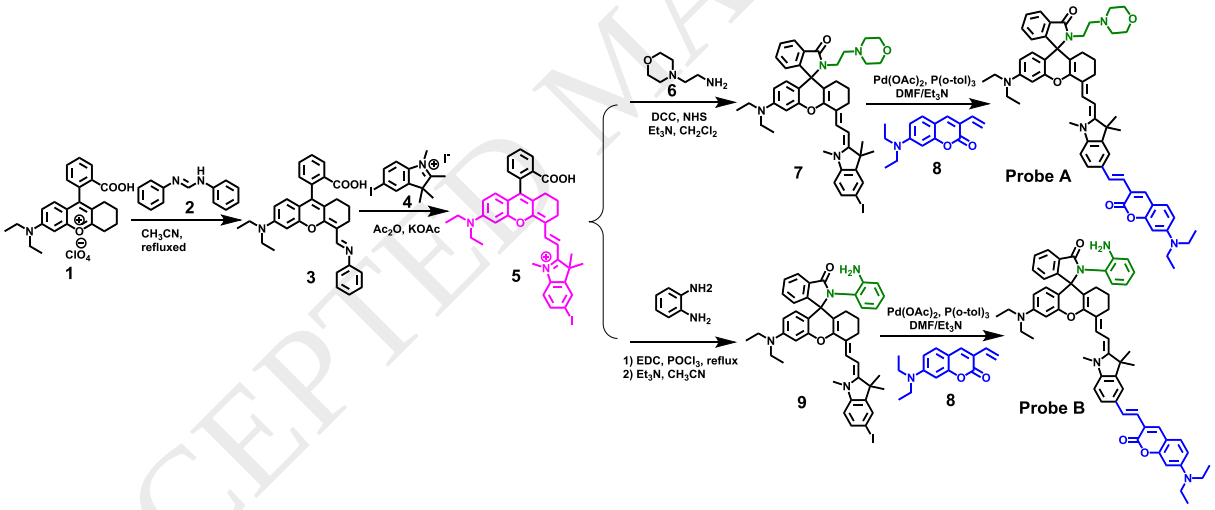

Scheme 2. Synthetic strategy to prepare a ratiometric fluorescent probes based on π-conjugation modulation between coumarin and hemicyanine dyes.